

Meso-scale effects of tropical deforestation in Amazonia: preparatory LBA modelling studies

A. J. Dolman¹, M. A. Silva Dias², J-C. Calvet³, M. Ashby¹, A. S. Tahara⁵, C. Delire³
P. Kabat¹, G. A. Fisch⁴, C. A. Nobre⁵

¹DLO Winand Staring Centre, Wageningen, the Netherlands
E-mail: dolman@sc.dlo.nl

²University of Sao Paulo, Sao Paulo, Brazil

³Meteo France/CNRM, Toulouse, France

⁴Centro Tecnico Aerospacial, Sao Jose dos Campos, Brazil

⁵Centro de Previsao de Tempo e Estudos Climaticos, INPE/CPTEC, Cachoeira Paulista, Brazil

Received: 4 September 1998 / Revised: 4 December 1998 / Accepted: 17 December 1998

Abstract. As part of the preparation for the Large-Scale Biosphere Atmosphere Experiment in Amazonia, a meso-scale modelling study was executed to highlight deficiencies in the current understanding of land surface atmosphere interaction at local to sub-continental scales in the dry season. Meso-scale models were run in 1-D and 3-D mode for the area of Rondonia State, Brazil. The important conclusions are that without calibration it is difficult to model the energy partitioning of pasture; modelling that of forest is easier due to the absence of a strong moisture deficit signal. The simulation of the boundary layer above forest is good, above deforested areas (pasture) poor. The models' underestimate of the temperature of the boundary layer is likely to be caused by the neglect of the radiative effects of aerosols caused by biomass burning, but other factors such as lack of sufficient entrainment in the model at the mixed layer top may also contribute. The Andes generate patterns of subsidence and gravity waves, the effects of which are felt far into the Rondonian area. The results show that the picture presented by GCM modelling studies may need to be balanced by an increased understanding of what happens at the meso-scale. The results are used to identify key measurements for the LBA atmospheric meso-scale campaign needed to improve the model simulations. Similar modelling studies are proposed for the wet season in Rondonia, when convection plays a major role.

Key words. Atmospheric composition and structure (aerosols and particles; biosphere-atmosphere interactions) · Meterology and atmospheric dynamics (mesoscale meterology)

Introduction

Modelling studies with general circulation models have shown that large-scale deforestation of the Amazon basin may result in increased surface temperatures and decreased rainfall (e.g. Lean and Rountree, 1993). This result is obtained because the modelled deforestation reduces evaporation and increases longwave outgoing and sensible heat fluxes, and consequently induces a drying of the planetary boundary layer (Sud *et al.*, 1996). Moreover, decreased large-scale convergence of moisture, caused by reduced aerodynamic roughness of the pasture compared to forest, also results in less precipitation. Typically, decreases amount to 10 to 20% of the annual rainfall.

The GCM results suggest that the climatological and hydrological effects of deforestation are a mixture of meso- γ to β scales and macro- β to α scale processes (Orlanski, 1975). Experiments with meso-scale models have shown that increased heating of the boundary layer may also trigger convection, if the initial moisture availability is sufficiently large (Avissar and Liu, 1996). Thus, according to their study, regional deforestation, leading to heat islands of pasture in an otherwise moist rainforest environment, may lead to enhanced rainfall (e.g. Silva Dias and Regnier, 1996). Enhancement of rainfall following deforestation has also been found in some GCM studies (e.g. Polcher, 1995). As deforestation does not affect the whole of the Amazon basin as yet, but is concentrated in regions such as Rondonia or Para, there is a clear need to understand the interplay between the micro-, meso-, and macro-scale processes, particularly with regard to rainfall generation. The physical climate component of the Large Scale Biosphere Atmosphere Experiment in Amazonia (LBA) (Nobre *et al.*, 1996a) is designed to provide this knowledge. LBA aims to generate enhanced understanding of the way Amazonia functions as a regional entity and how this may change under global climate change and human induced land use changes.

The key questions to be addressed in the meso-scale field campaigns of LBA (Nobre *et al.*, 1996a) are: what are the meso-scale mechanisms by which differences in surface characteristics translate into large-scale weather anomalies and what is the role of dry and moist convection in transferring energy and how will this change with different land use patterns?

To prepare this experimental programme a modelling study was initiated to identify the main uncertainties in the current understanding of the effects of tropical deforestation at the meso scale (Dolman *et al.*, 1993). The study consists of collection of available data, and use of these in state-of-the-art meso-scale models to bring out the major areas of uncertainty in the model predictions. Collection of land surface data and topography is described in Calvet *et al* (1997).

Experimental evidence from previous studies suggest that meso-scale circulations caused by large water bodies such as the Amazonian rivers, may lead to significant small-scale rainfall gradients (Martin *et al.*, 1988). Furthermore, the Rondonia Boundary Layer Experiments II and III have provided the first experimental evidence of large differences between the structure and growth of the boundary layer over forest and pasture (Fisch, 1996). During the dry season, simultaneous measurements of boundary layer temperature and humidity show that the boundary layer over the pasture is between 500 to 1000 m deeper and up to 2 K warmer. Although to a large extent these differences are related to differences in surface heating (see e.g. Wright *et al.*, 1992), existing slab models of the boundary layer development fail to predict the correct growth when fed with observed surface heat fluxes for deforested areas (Fisch *et al.*, submitted 1997).

As the boundary layer plays a key role as mediator between the surface and large-scale weather systems, it is of obvious importance to correctly model and understand the mechanisms involved in the boundary layer growth of the Amazonian dry season. This is even more so, as the drying predicted by GCMs will have the strongest ecological implications during the dry season, when rainfall is scarce, and most probably of local origin (Cutrim *et al.*, 1995).

The current work describes the modelling programme initiated as preparation for the LBA meso-scale field campaigns. The focus of current studies is on processes in the boundary layer and the large-scale influence of the Andes. It is emphasised that the purpose

of this study is to highlight existing model deficiencies to aid setting the modelling and experimental priorities for LBA, not necessarily to correct these deficiencies at this stage. The regional atmospheric modelling system (Pielke *et al.*, 1992) and a 1-D version of the newly developed French non-hydrostatic meso-scale model MESO-NH are used to highlight some of the model deficiencies. The 3-D model is run in two nested configurations with different grid lengths to investigate surface atmosphere interaction at the relevant spatial scales. The models are run for selected days periods during the 1994 dry season in Rondonia. During this period the third Rondonia Boundary Layer Experiment took place, and surface flux data are available from the joint Brazilian-UK ABRACOS (Anglo Brazilian Climate Observation Study) experiment (Gash and Nobre, 1997). The 1-D model is used to highlight particular difficulties in modelling aerosol behaviour in the boundary layer. It is one of the few meso-scale models with a parametrisation of aerosols in the boundary layer.

Models

The main features of the two models used are summarised in Table 1. RAMS (the regional atmospheric modelling system) has been developed at Colorado State University. The two major components in RAMS are the data analysis and assimilation package and the atmospheric model. The former allows the use of meteorological observations and/or analyses from larger scale models for initialisation and model 'nudging'. The atmospheric model is based around the full set of primitive dynamical equations governing atmospheric motion. These equations are supplemented by optional parametrisations for long- and short-wave radiation, turbulent diffusion, moist processes, surface-atmosphere moisture and energy exchange, kinematic effects of terrain, and cumulus convection (Pielke *et al.*, 1992). The land surface scheme models the heat and moisture exchange between the atmosphere, vegetation canopy, multiple soil layers and surface water (Avissar and Pielke, 1989). Two-way interactive grid nesting allows simultaneous modelling of physical processes at variable length scales.

MESO-NH is a regional area model developed recently, used here in 1 D simulations only, to highlight some of the modelled boundary layer behaviour. The

Table 1. Characteristics and main differences between the models

	Grid length (km)	Domain size (km)	Day (1994)	Surface scheme	Surface classification	Soil classification
RAMS Meso- γ	16–2	270*270	16–19 August	Avissar and Pielke (1989)	Landsat	Single soil type
RAMS Meso- β	60–20	2400*2400 880*880	15–18 August	Avissar and Pielke (1989)	All forest	Single soil type
MESO-NH	1-D only	n/a	18 August	ISBA	Derived from Landsat RADAM BRASIL	Derived from RADAM BRASIL

full design is discussed in Lafore *et al.* (1998). The model integrates the non-hydrostatic anelastic equations using finite-differences techniques for the spatial and temporal discretizations. The upper boundary of the model is a rigid top with a sponge layer, whereas the lower boundary conditions are provided by the ISBA surface scheme (Noilhan and Planton, 1989). MESO-NH also includes a turbulence scheme based on the turbulent kinetic energy parametrisation of Bougeault and Lacarrere (1989), a subgrid-scale condensation scheme of the boundary layer based on Sommeria and Deardorff (1977), and a sophisticated radiation code (Morcrette, 1989).

Data

A substantial data set consisting of forcing from large-scale analysis, surface maps and boundary layer and flux data was assembled. Analyses from both the European Centre for Medium Range Weather Forecasting and from the National Centres for Environmental Prediction (NCEP) are used as forcing for MESO-NH and RAMS respectively.

The large-scale situation over Central Brazil and Amazonia around the days of simulation August 19–21, 1994 is depicted in Fig. 1 from the NCEP analysis. The geopotential field at 500 hPa shows a ridge with a few

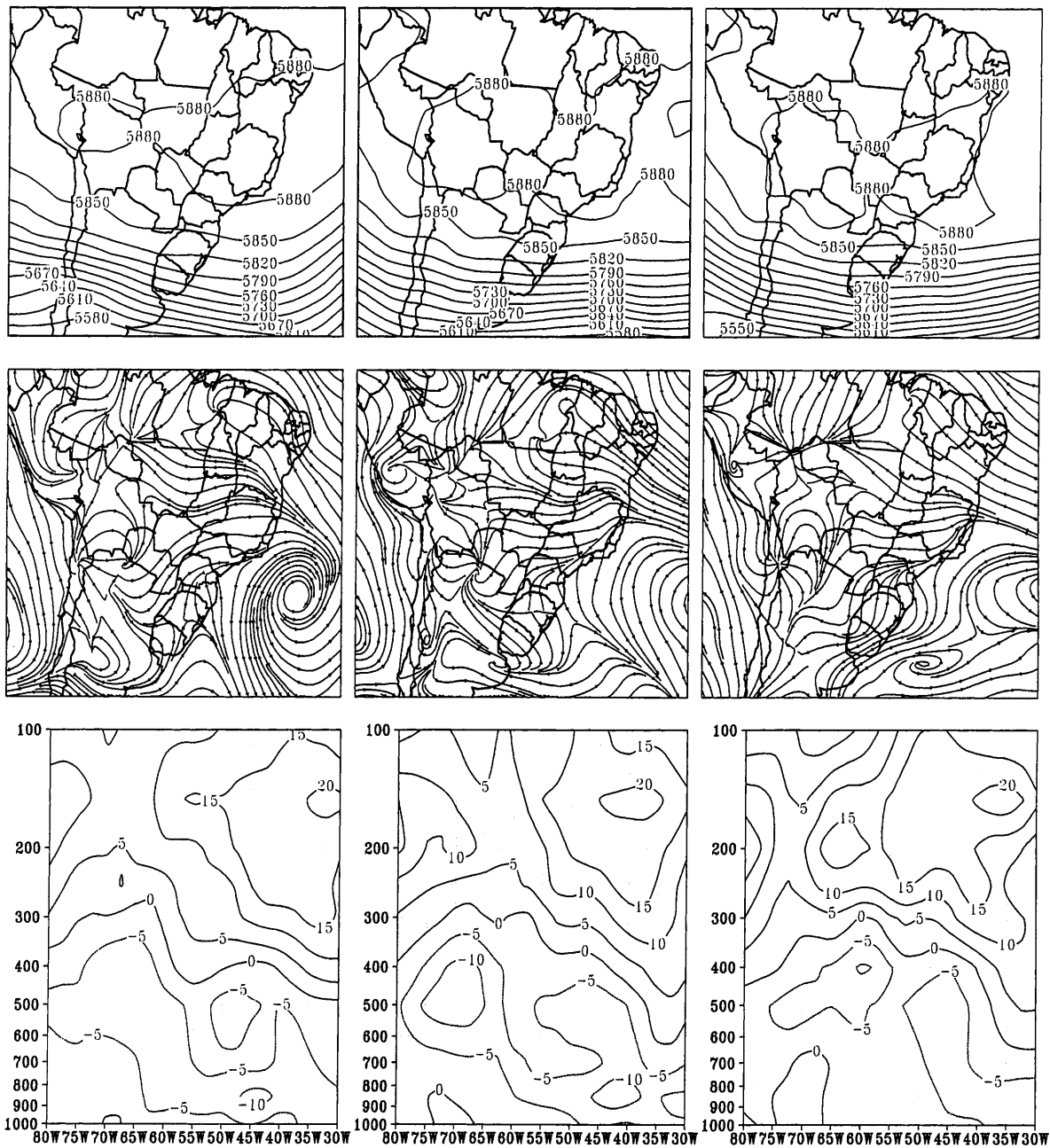


Fig. 1. Upper panel: 500 hPa geopotential; middle: streamlines at 1000 hPa; lower: vertical cross section along 12.5°S of the zonal wind component. Columns from left to right: 19, 20 and 21 August, 1994, 12 UTC

short waves in the southern part. A short wave trough enters northwestern Argentina on the 19th of August, moving eastwards during the following days. This disturbance, however, does not produce any significant variation in the wind field in lower levels (1000 hPa) in Rondonia, also shown in Fig. 1. Winds remain from the southeast in the eastern part of Rondonia turning to northwest in the western part. A vertical cross section through 12.5°S shows the zonal wind component (lower panel in Fig. 1). Easterly winds prevail in the lower troposphere. In upper levels, above 400 hPa, winds are from the west. During the August 19–21 period upper level winds over Rondonia accelerate from 5 to 15 m s⁻¹.

According to Horel *et al.* (1989) and Mohr and Zipser (1996), among others, convection over South America in the dry season of central Amazonia shifts to the northwest of the Amazon Basin. The upper level situation in these cases responds with an anticyclonic circulation centred close to the region of convective activity, and the southern border produces a variability of westerlies in upper levels over tropical Brazil in response to the variability of convection in the northwestern side of the Basin. The simulations over Rondonia thus show the typical characteristics of the higher and lower level synoptic situation associated with the dry season.

Land surface classification maps were derived from 1993–94 LANDSAT-TM data. Soil and natural vegeta-

tion maps over Rondonia (600 × 600 km) at the 1:1 000 000 scale from the project “Levantamento dos recursos naturais” were obtained in Brazil at the Fundacao Instituto Brasileiro de Geografia e Estatistica (IBGE). Topography is also available at both the 1:1 000 000 and 1 : 250 000 scale. Topography data were digitised to produce maps for use in the meso scale models. Figure 2 shows the LANDSAT classification overlaying a vegetation map. Details of the way the data was acquired and processed can be found in Calvet *et al.* (1997). Figure 3 shows a histogram of the percentage forest cover for a 600*600 km domain at 10 km grid length. It is noteworthy that in the deforested areas the percentage pasture rarely exceeds 60% of the total cover, indicating that, what is called pasture for a meso-scale model grid box, is in reality a mixture of pasture and forest.

Surface fluxes of radiation, sensible and latent heat were measured during the ABRACOS project (Gash and Nobre, 1997) at a forest site in the Reserva Jaru (RJF), near Ji Parana in Rondonia State, Brazil (10° 05'S, 61° 55'W) and a deforested site near Ji Parana, the Fazenda Nossa Senhora (NSP) (10° 45'S, 62° 22'W). Note that the words pasture and deforested area do not necessarily mean the same, although their use here is somewhat interchangeable. For surface fluxes a pasture area refers to pure pasture, i.e. grassland with stumps of burnt trees (e.g. Wright *et al.*, 1992). In terms of boundary layer development, a much larger area is

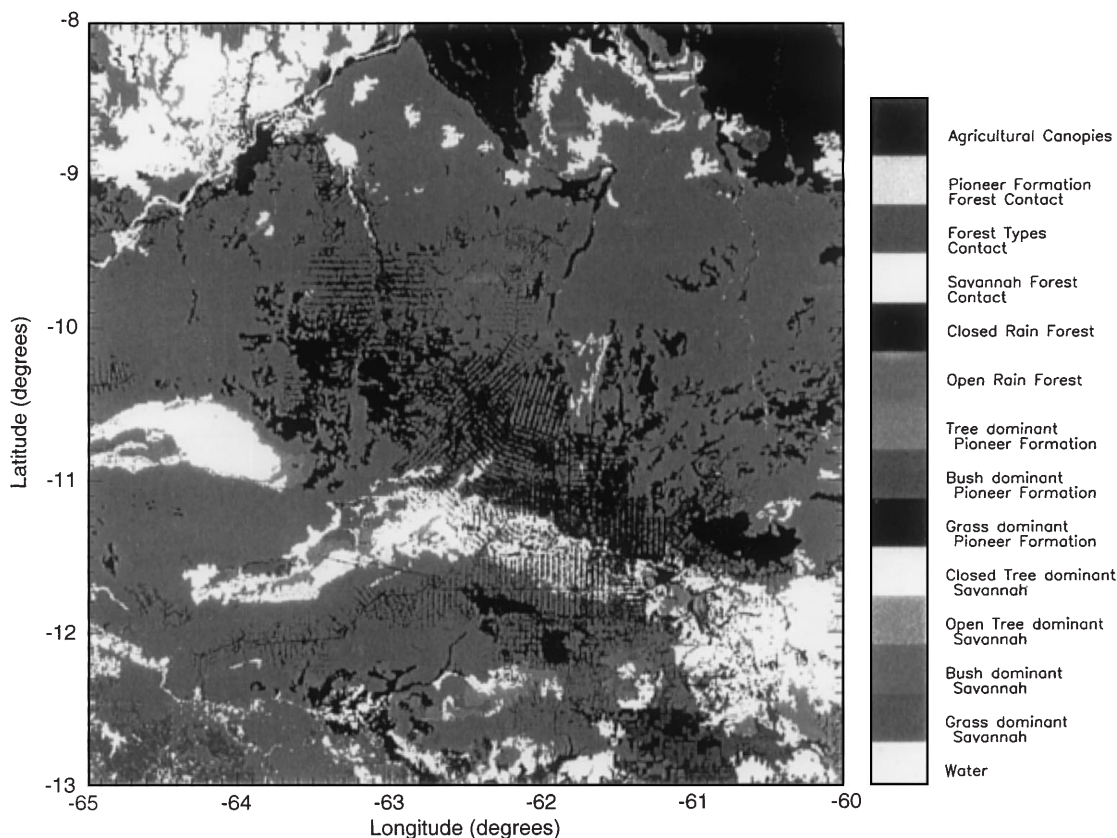


Fig. 2. Land cover classification derived from LANDSAT imagery and RADAMBRASIL vegetation classification

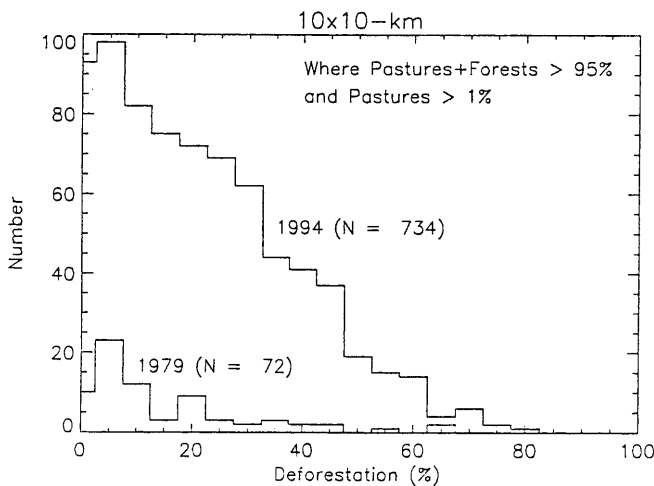


Fig. 3. Histogram of the deforestation rate in 1993–1994 as calculated for a 10 km × 10 km grid from the 120-m pixel size map produced over the 8–13 S, 60–65 W domain. The histogram obtained for 1979 from the RADAMBRASIL maps (Calvet *et al.*, 1997) is also plotted

implied; here areas of pure pasture are interspersed with patches of untouched forest.

Simultaneous radiosonde and tethered balloon measurements were made at the forest and pasture site during the Rondonia Boundary Layer Experiment III (RBLE-III) during the 1994 dry season (August 13–25). The data have been collected simultaneously at the forest and pasture sites of ABRACOS around the Ji-Paraná region (Gash and Nobre, 1997). The radiosoundings were made at 5:00, 8:00, 11:00, 14:00, 17:00 and 23:00 local time. The evolution of the nocturnal boundary layer was studied by measurements with a tethered balloon at 18:00, 19:30, 21:30, 24:00, 5:30, 7:00 and 8:30 LT. A detailed description of the experimental design and the observational aspects can be found in Fisch *et al.* (submitted 1997).

Calibration of land surface schemes

The RAMS land surface scheme is based on Avissar and Pielke (1989). For the runs with the meso-scale model in this part of the project it was decided not to change the land surface parametrisation, but to calibrate the scheme so that it reproduced correctly the observed fluxes for the days of interest. This procedure is acceptable for simulation periods of the order of a few days, but would become unreliable if longer runs were made and vegetation phenology and/or soil moisture changes. The state of the art of land surface models unfortunately is still such that running a land surface model without calibration for a new vegetation type initially generates unrealistic simulations. The Amazon applications as described here present no exception to this general rule (e.g. Delire *et al.*, 1998).

The scheme allows for bare soil and vegetation to exist jointly. The latent heat flux is described as a function of the relative stomatal conductance, which is a function of global radiation, leaf temperature, vapour

pressure difference between the leaf and air and soil water potential. In the present case the dependence of the relative stomatal conductance on soil water content is calibrated to obtain agreement with the observed fluxes for the two vegetation classes. In the equation describing the soil moisture-conductance relation a factor is introduced which allows calibrating the scheme against observed fluxes.

Figure 4 shows the comparison between observed and simulated shortwave radiation, latent and sensible heat fluxes for 19–21 August for the pasture (Nossa Senhora, NSP) and forest (Reserva Jaru, RJF) site. As the simulations are made for the dry season, biomass burning causes a considerable aerosol loading of the atmosphere over the pasture areas. Although, the source of the smoke is located primarily in the pasture and newly burnt forest areas, it is to be expected that over the untouched forest areas, the aerosol content would also be high. These effects are not accounted for in the models.

Thus, initially the modelled shortwave radiation above both the forest and the pasture was too high. The shortwave downward radiation flux is therefore calibrated by reducing the solar constant by 15% to give the correct surface shortwave at the forest site. This gave the correct radiation flux surface at the forest surface, but obviously does not account for any scattering and absorption of radiation in the boundary layer. However, the measured shortwave downward flux at the pasture is lower than the forest shortwave by about 100 W m⁻² at noon. In the simulations the difference between modelled

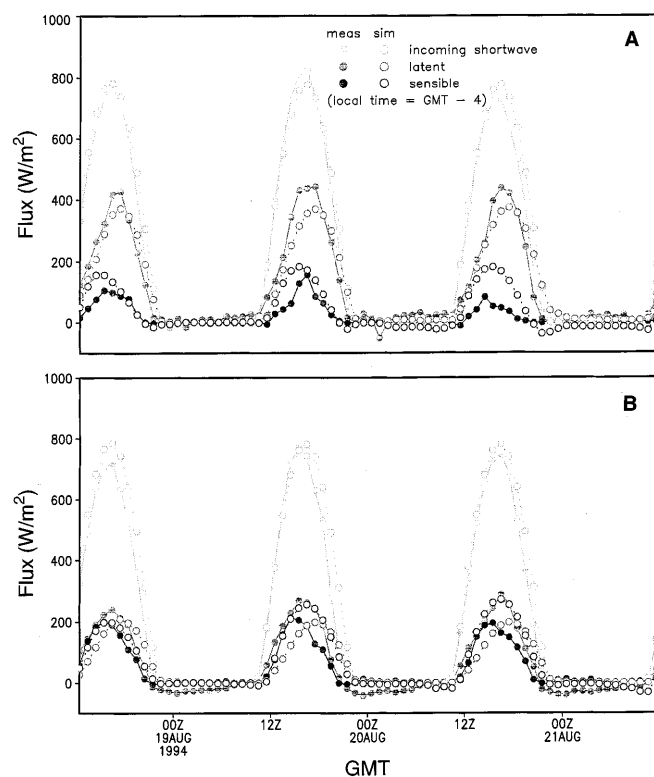


Fig. 4A, B. Comparison of modelled and observed incoming shortwave radiation, latent and sensible heat flux for **A** forest and **B** pasture for the RAMS land surface model

and measured shortwave is therefore greater at the pasture site than at the forest site. Given the uncertainty in modelling radiation absorption, and the spatial distribution of aerosols over the area, it was decided to use the same reduction factor for pasture and forest.

Given the approximately correct shortwave down, the fluxes of latent and sensible heat can be simulated to a level of acceptable accuracy for the few days of simulation. At the NSP site the latent and sensible heat fluxes are roughly of equal magnitude with maximum levels of about 200 W m^{-2} . This partitioning of available energy is well captured by the scheme. For the RJF site the latent heat component is the larger term in the energy balance and again this is well simulated by the land surface scheme. Sensible heat is the smaller component of the energy balance with a peak value of 100 W m^{-2} . Maximum latent heat fluxes of about 400 W m^{-2} are well simulated. The parameters used in this study are given in Table 2.

Most of the ISBA parameters (see Noilhan and Planton, 1989 for a full description of the model equations) are fixed by measurements (see Table 3). The only parameters to be calibrated are the minimum stomatal resistance R_{smin} , the vegetation heat transfer coefficient C_v and the ratio of the roughness lengths for momentum and heat z_{0m}/z_{0t} . In the present case, this ratio is fixed to a value of 10. The calibration is performed with the adapted version of ISBA, taking into account the hydrological properties of the Amazonian soils as derived by Delire *et al.* (1997). The flux measurements used to calibrate ISBA were collected during the intensive field campaigns of ABRACOS (Gash *et al.*, 1996). The data consist of hourly estimates of net radiation R_n , soil heat flux G , sensible heat flux H and latent heat flux λE . The soil heat flux G is used to calibrate C_v and R_{smin} is calibrated with the fluxes. The calibrations of C_v and R_{smin} are thus independent. Data from the various missions at a single site are treated consecutively as if they were part of a single data set. Except for RJF where soil moisture measurements are

limited to a depth of 3.6 m, the soil moisture content in the model was re-initialised to the observed value at the beginning of each mission. The time step used for each run is 300 s. For RJF, the simulated soil heat flux is compared to the residual of the observed energy balance which is not identical to the measured soil heat flux because of the heat storage in the canopy. ISBA considers only one energy balance for the whole ground-vegetation system. As a result, the simulated soil heat flux represents the total heat flux entering the vegetation, the canopy air and the soil.

Optimised values of C_v and R_{smin} are given in Table 3. Calculated versus observed values of the surface fluxes for the forest site are presented in Fig. 5. The agreement is good. Further details on the calibration, especially on the derivation of Amazonian soil properties for ISBA may be found in Delire *et al.* (1998). These soil hydraulic properties are crucial in our understanding of long term surface atmosphere interaction and adequate prediction of long term, seasonal trends of soil moisture during the dry and wet season.

1-D modelling

Earlier work (Fisch, 1996) has shown that a marked difference can exist between the growth characteristics of the boundary layer over forest and pasture. The structure and time evolution of the Amazonian boundary layer at Ji-Parana has been observed during the RBLE-II (Nobre *et al.*, 1996b). Observations show that over forest the convective boundary layer grows up to a height of 1000–1200 m, whilst, over the pasture the final depth could be up to 2000 m. It is to be expected that this change in final depth is primarily the result of differences in sensible heat fluxes from surface.

Over both the pasture and forest sites, the clear sky boundary layer is simulated for 18 August, 1994, from 0500 LST (the 0500 LST radio soundings are taken as the initial condition) to 1700 LST, with a time step of

Table 2. The RAMS scheme soil and vegetation structure parameters over the Rondônia sites of ABRACOS during the dry season. The values are either prescribed, measured, calculated from continuous functions of the texture, or calibrated

Symbol	Definition	RJF	NSP	Unit	Source
Soil parameters					
Clay fraction		0.8	0.8		Prescribed
Sand fraction		0.18	0.18		Prescribed
b	Clapp and Hornberger b	10	10		Prescribed
k_s	Thermal conductivity	$2.34 \cdot 10^{-7}$	$2.34 \cdot 10^{-7}$	m^2/s	Measured
$k\theta_s$	Sat. hydraulic cond	$2.6 \cdot 10^{-3}$	$2.6 \cdot 10^{-3}$	m/s	Measured
σ_{cp}	Heat capacity of dry soil	$1344 \cdot 10^3$	$1344 \cdot 10^3$	$\text{J/m}^3/\text{K}$	Prescribed
σ_s	Density of wet soil	1600	1600	kg/m^3	Prescribed
θ_s	Porosity	0.4	0.4	m^3/m^3	Measured
$-s$	Sat. moisture potential	-0.5	-0.5	m	Measured
Vegetation parameters:					
LAI	Leaf Area Index	5.6	3	$\text{m}^2 \text{ m}^{-2}$	Measured
α	Vegetation coverage	95	85	%	Measured
	Albedo	0.14	0.19	—	Measured
ε	Emissivity	0.95	0.95	—	Prescribed
z_0	Roughness length	2.35	0.053	m	Measured
a	Factor soil moisture stress	0.07	0.01	—	Calibrated

Table 3. The ISBA scheme soil and vegetation structure parameters over the Rondônia sites of ABRACOS during the dry season. The values are either prescribed, measured, calculated from continuous functions of the texture, or calibrated

Symbol	Definition	RJF	NSP	Unit	Source
Soil parameters:					
d_2	Soil root depth	8	2	m	Prescribed
CLAY	Clay fraction	24	30	%	Measured
SAND	Sand fraction	63	60	%	Measured
w_{wilt}	Wilting point	0.16	0.18	$\text{m}^3 \text{ m}^{-3}$	Continuous functions
w_{fc}	Field capacity	0.28	0.30	$\text{m}^3 \text{ m}^{-3}$	Calibrated functions
w_{sat}	Saturation	0.39	0.40	$\text{m}^3 \text{ m}^{-3}$	Continuous functions
Vegetation parameters:					
LAI	Leaf Area Index	4.6	1.5	$\text{m}^2 \text{ m}^{-2}$	Measured
veg	Vegetation coverage	99	85	%	Measured
	Albedo	0.14	0.20	—	Measured
C_V^s	Emissivity	0.95	0.95	—	Prescribed
r_{smin}	Thermal coefficient	1.2×10^{-5}	5.0×10^{-3}	$\text{Km}^2 \text{ J}^{-1}$	Calibrated
	Minimum stomatal resistance	175	132	sm^{-1}	Calibrated
	Vapour pressure deficit sensitivity	0.04	0.	kg kg^{-1}	Prescribed
R_{GL}	Global radiation limit	30	100	Wm^{-2}	Prescribed
z_0	Roughness length	2.6	0.06	m	Calibrated
z_0/z_{0h}	Roughness length ratio	10	10	m m^{-1}	Prescribed

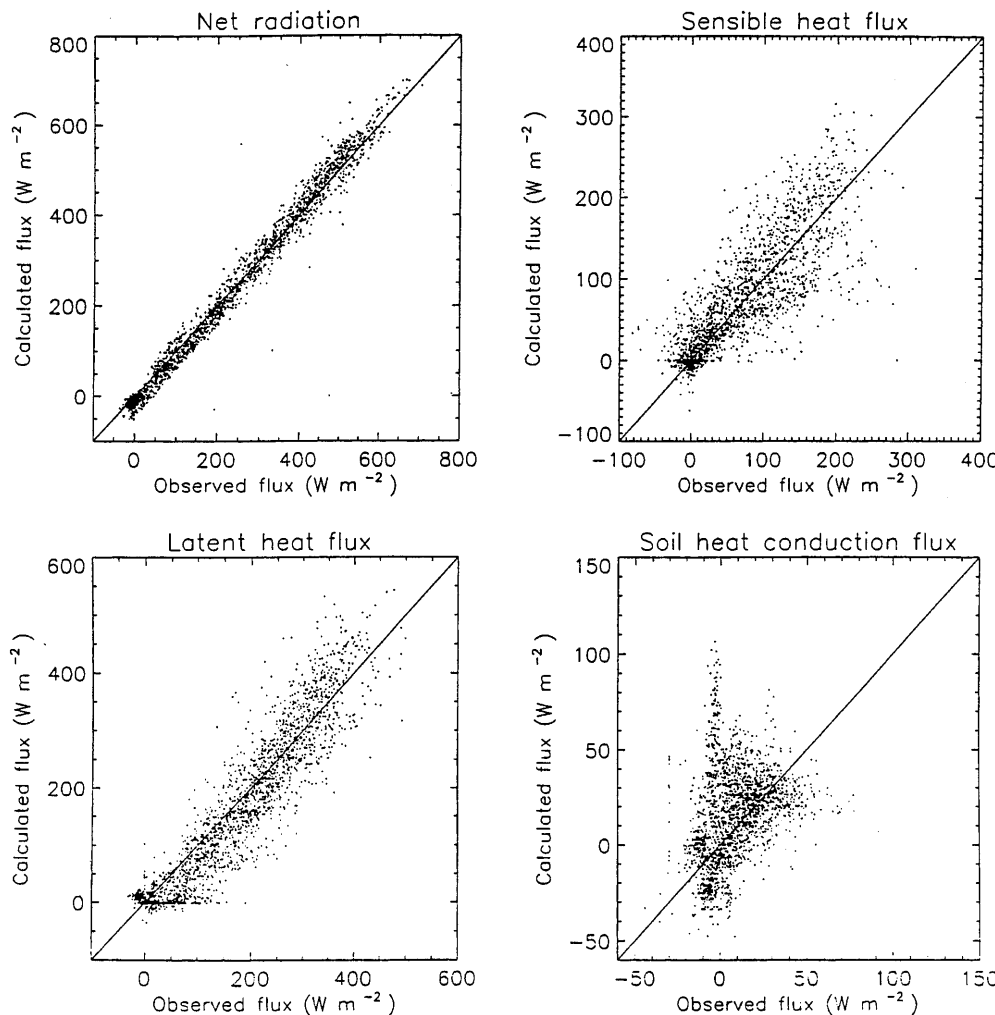


Fig. 5. Comparison of modelled and observed net radiation, latent and sensible heat flux and soil heat flux for forest for the ISBA land surface model

60 s and a constant vertical resolution $\Delta z = 35$ m. The simulations can be compared with the RBLE-3 measurements every three hours. Initially, 10 km \times 10 km maps suitable for runs with a meso-scale model were produced from the high resolution digital maps (Calvet *et al.*, 1997) of soil and natural vegetation and from the 1993–1994 LANDSAT classification for Rondônia. The required change in pixel size from the original digitised pixel size was obtained by applying simple aggregation rules (Noilhan *et al.*, 1997). The surface properties (i.e. the ISBA parameters) used in the 1-D runs are those obtained for the gridpoints covering RJF and NSP and correspond to 100% and 60% forest cover and 0% and 40% pasture respectively. The average textural properties of the sites and the corresponding soil characteristics are presented in Table 3.

From the surface solar radiation (R_g) measurements and preliminary simulations with MESO-NH, it appeared solar radiation was not well predicted. Since the simulations are performed for the biomass burning season, it was thus assumed that a large part of the solar radiation was absorbed by aerosols. From those initial simulations, the estimated optical thickness of the aerosols on August 18, 1994 is 0.20 for RJF and 0.25 for NSP at 1200 LST. In the simulations presented here, the effect of radiation absorption by aerosols is taken into account by assuming an aerosol profile that has a distribution proportionally similar to that of specific humidity in the boundary layer. The aerosol optical thickness at the altitude z is expressed as:

$$\tau_{aer}(t, z) = aq_a(t, z)\delta z$$

where q_a is the simulated specific humidity at time t and level z , and a a coefficient to be calibrated. In the

simulations, the aerosol properties (single scattering albedo and extinction coefficient) correspond to a standard continental aerosol class. The estimated value of a on August 18, 1994 which produced a good shortwave downward radiation flux at the surface is 0.0429 and 0.0543 m $^{-1}$ for RJF and NSP, respectively.

Figure 6 presents the simulated and observed humidity and temperature profiles over the two sites at 1700 LST. Over RJF (Fig. 6A, B), the boundary layer height of about 1000 m is well simulated, although the humidity is slightly overestimated. On the other hand, the boundary layer height of NSP is significantly underestimated (the model predicts a boundary layer height of 1600 m whereas the observed value is about 2200 m). Again, the humidity within the boundary layer is slightly overestimated. Figure 7 shows more details about the simulations by comparing the surface fluxes are against the measurements. The agreement between the measured and simulated surface fluxes is good for RJF (not shown). For the pasture site, NSP (Fig. 7), the simulated aggregated sensible heat flux is somewhat higher in the morning than the measured value and lower in the afternoon. This is because the aggregated heat flux represents the combined effect of the pasture and forest stripes, whereas the measured value represents only the pasture *sensu stricto*. The latter does not involve remaining forest areas in the pasture fields which would act to bring down the value of sensible heat.

Meso- γ scale modelling

RAMS was run in non-hydrostatic mode over an area in Rondonia with two nested grids in a larger domain.

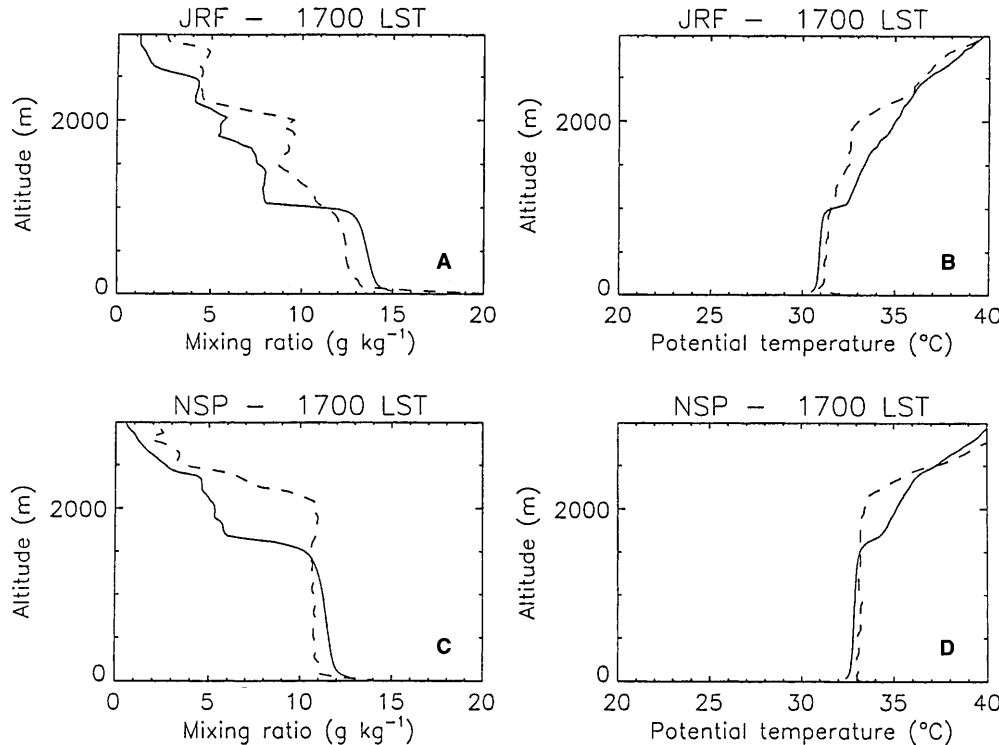


Fig. 6A–D. Simulated (solid line) and observed (dashed line) vertical profiles of **A, C** humidity mixing ratio, and **B, D** potential temperature at 1700 LST, over **A, B** undisturbed forest and **C, D** 60% deforested sites of Rondonia for August 18, 1994 from MESO-NH

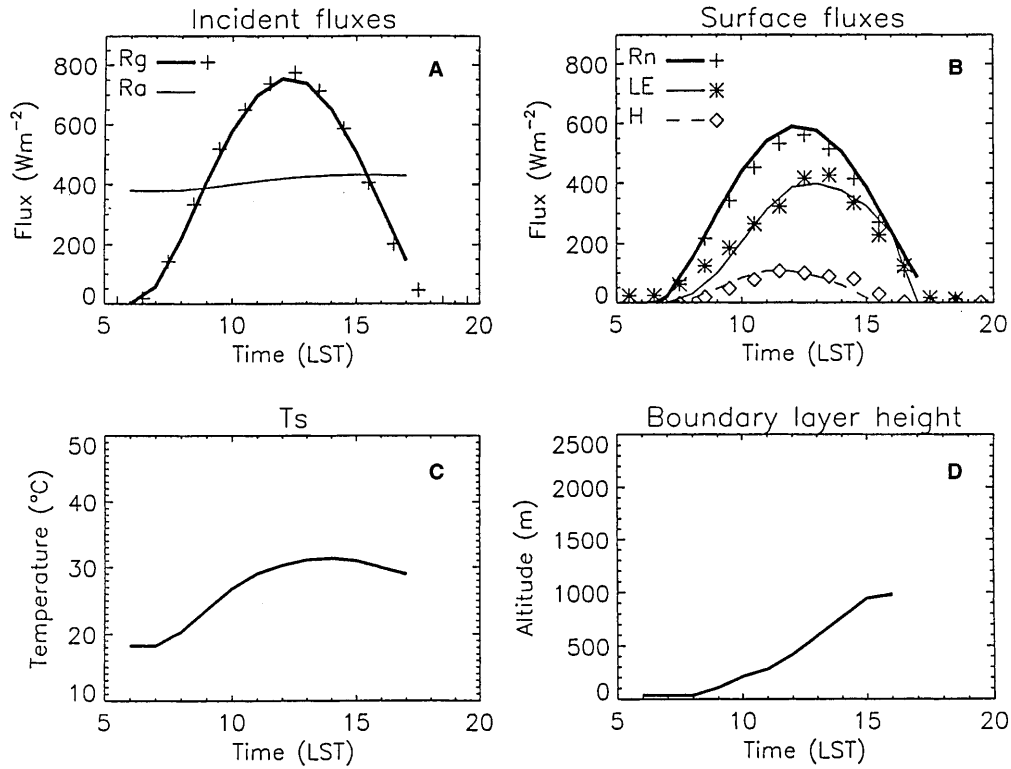


Fig. 7A–D. Simulated parameters over the 60% deforested site (NSP): **A** incident solar (R_g) and atmospheric (R_a) radiation, **B** surface net radiation (R_n), evapotranspiration (LE), and heat flux (H), **C** surface temperature (T_s), and **D** boundary layer height from MESO-NH. The observed values are indicated by points

The grid length of the largest domain is 16 km, that of the smallest 1 km. A schematic of the model configuration indicating the areas of pasture and forest is shown in Fig. 8. The land surface classification for RAMS is obtained from the LANDSAT-TM classification (Calvet *et al.*, 1997). This classification is degraded from 30 m to the required model grid length

(16, 4 and 1 km) by taking the predominant cover class. The number of levels in the vertical is 31, the lowest layer 50 m deep and the top of the model is set at 16 000 m. The lateral boundary condition is derived from Klemp and Wilhemson (1978). Nudging at the lateral and top boundaries takes place at the 5 most exterior grid point laterally, with six and one hour time

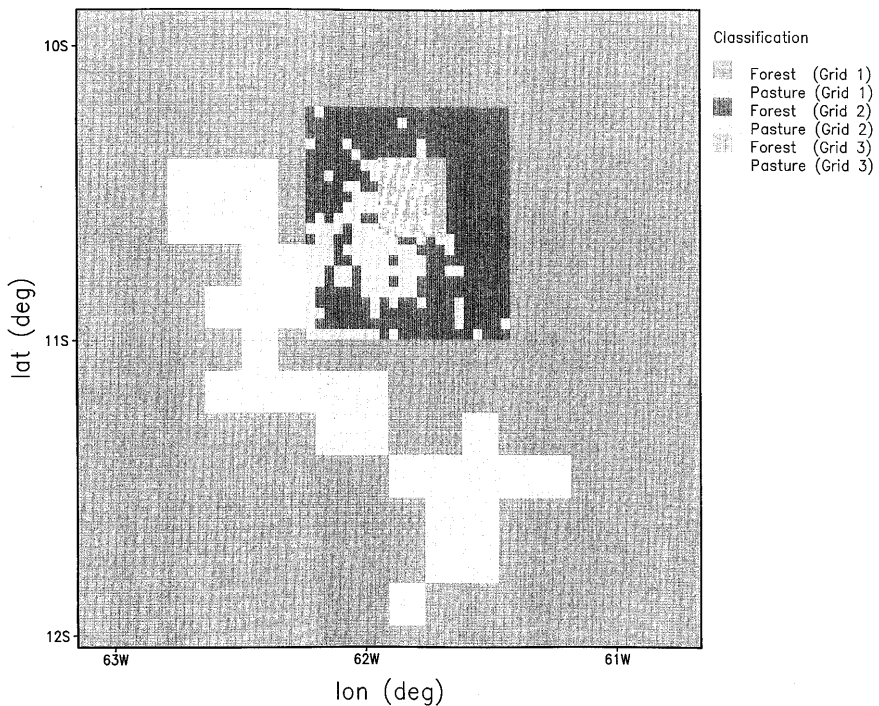


Fig. 8. Nested simulation domains for the RAMS model

scales respectively towards the large scale analysis of NCEP at 2.5° by 2.5° . At the centre of the domain, no large-scale forcing is imposed and the model follows its own behaviour. Radio sonde data over the forest and NCEP data are used to initialise the model. The model is integrated forward for 18, 19 and 20 August, 1994.

The simulation of the surface fluxes of latent and sensible heat of the RAMS land surface model has been dealt with above. Here it is sufficient to note that they are sufficiently close to the observations to assume that the input from a pasture or forest grid represents that particular homogeneous surface type only. In the current simulations, because of the fact that the nesting is assumed to resolve the heterogeneity, no aggregation of surface parameters was applied.

Figure 9 shows the boundary layer development for potential temperature over the RJF site and NSP sites.

Measurements are also shown. The agreement between the modelled and observed potential temperature profile over the RJF forest site is reasonable. This indicates that the large scale analysis of the NCEP model used for initialising and nudging is probably representative of the forest boundary layer. But, the final temperature is somewhat too low and after the initial development, the temperature profile drifts.

Over the pasture the modelled potential temperatures agree less well than over the forest. The simulated values are too cold in the morning and the final boundary layer depth is underestimated. Furthermore, the observations show a much warmer boundary layer, by up to 5° in the afternoon. Given that the sensible heat input from the surface is close to observations, this implies that the model does not provide enough heat input to the boundary layer from other processes. These may be entrainment of warmer air for above,

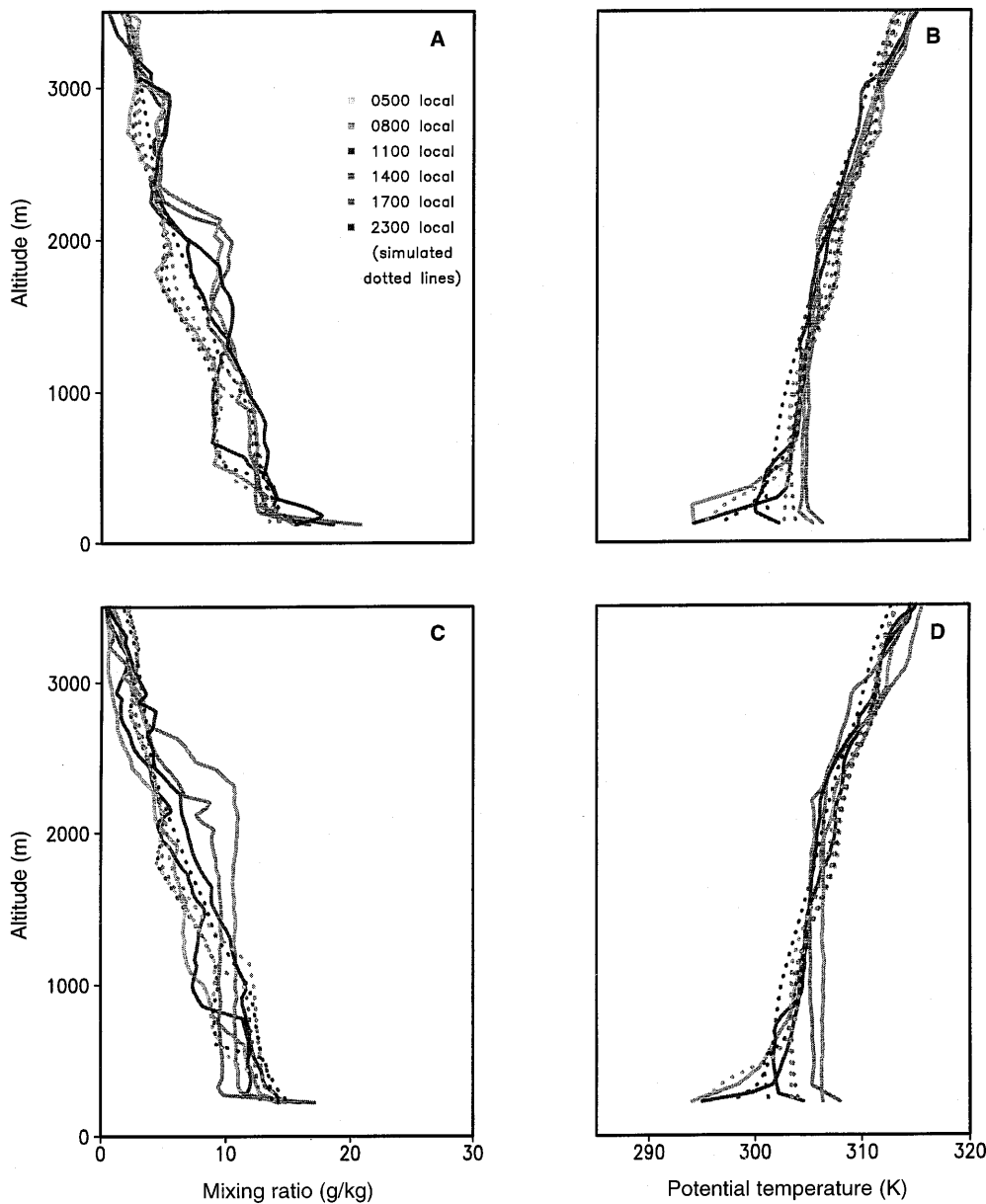


Fig. 9A–D. Simulated (dotted lines) and observed (solid lines) mixing ratio and potential temperature profiles for 18 August for **A, B** RJF and **C, D** NSP with the RAMS model

large-scale subsidence, horizontal advection or radiative absorption through aerosols. Horizontal advection was negligible. Lack of adequate mixing could also contribute to the lack of mixed layer heating, but an extra heat source would still have to present to add to the heat content of the boundary layer. The underestimation of both the temperature and depth makes it likely that a combination of aerosol absorption and entrainment is responsible for this.

It is possible by taking the boundary layer heat budget equation to estimate the potential contribution to boundary layer warming by aerosol absorption. At solar noon, this contribution may amount to almost 100 Wm^{-2} (Mattos *et al.*, 1996) and corresponding heating rates for a boundary layer of 1500 m deep are of the order of 0.2 K h^{-1} . Shallower boundary layers have higher heating rates, and thus the effect may be more pronounced in the early morning when boundary layer

experiences a rapid growth. This order of magnitude argument suggests that the lack of a treatment of the radiative effects of aerosols in the models could at least be partly responsible for the poor prediction of potential temperature over the deforested area and may also explain part of the disagreement of the observed and measured profiles over the forest.

The agreement between modelled and observed mixing ratio profiles is quite reasonable. This is shown in Fig. 9 and 10. The forest boundary layer is marginally wetter than the pasture boundary layer, in the measurements and somewhat less so in the simulations. The modelled boundary layers are both too wet and also appear to drift after initialisation.

The differential heating due to the surface transition of forest and pasture is also shown in Fig. 11 which shows patterns of sensible and latent heat. The pattern follows the typical fishbone pattern of vegetation

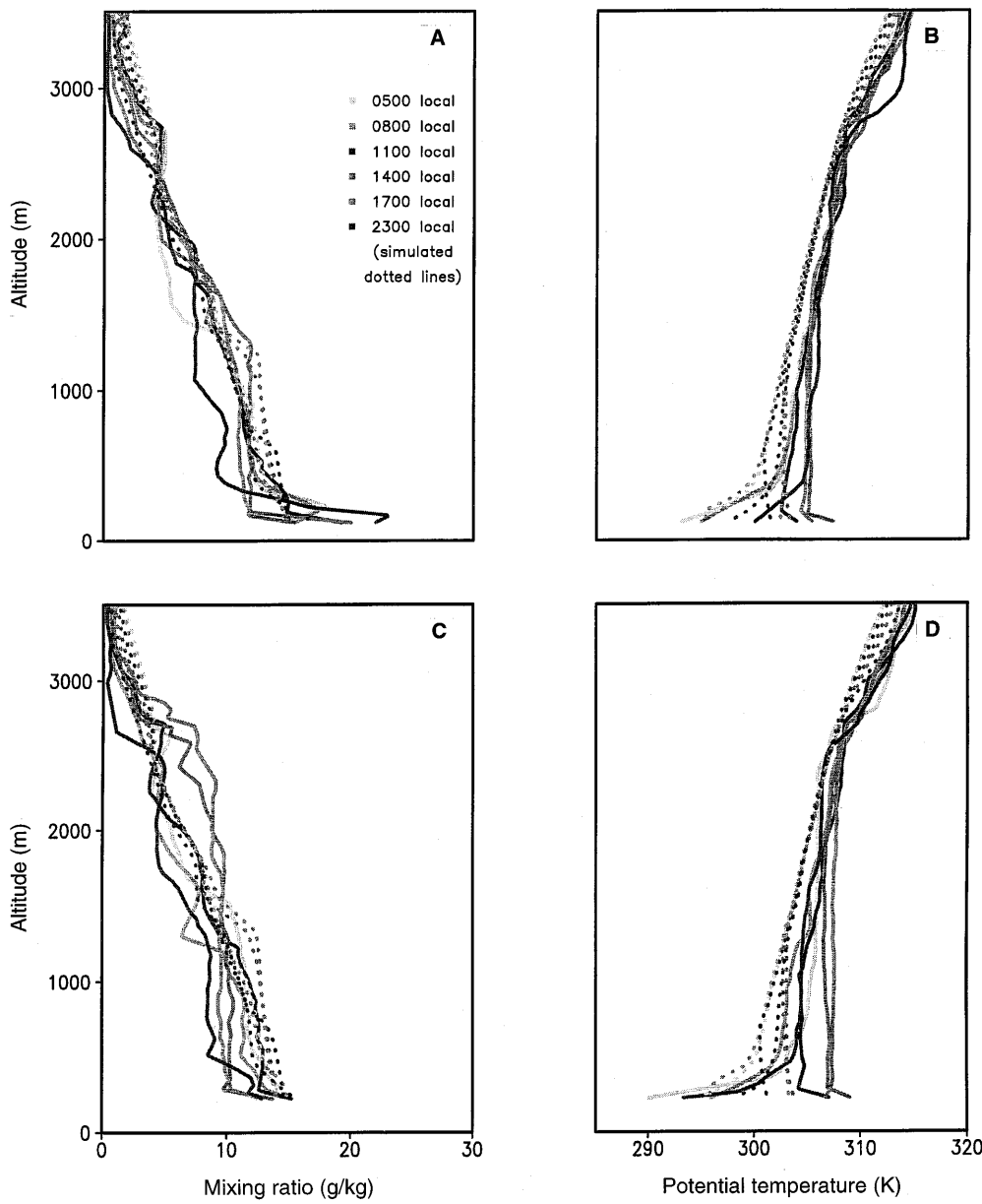


Fig. 10A–D. Simulated (dotted lines) and observed (solid lines) mixing ratio and potential temperature profiles for 19 August for **A, B** RJF and **C, D** NSP with the RAMS model

closely. The differential heating produces an effect in the distribution of the vertical velocity. As shown in Fig. 12 for 20 August 13.00 h, air is seen to be rising preferentially over the pasture and sinking over the forests. This would seem the beginning of a thermal circulation. The length scale of the circulations is relatively small and of the order of a few kilometres, consistent with the extent of the forest/pasture patches. At 17.00 h, the cell of rising air has moved westwards along with the main wind direction and lost its close relation with the vegetation type. The associated potential temperature difference between forest and pasture is about 1 K. Surface winds are of the order of 1–2 ms⁻¹. The circulations appear to be real vegetation induced, but according to the current simulations they eventually may decay or move across the domain. The effect of this on the overall domain wide turbulence, and vertical velocity remains to be investigated. It is worth emphasising that the level of the background wind will to a large extent determine the fate of the circulations. The current simulations are made with a background wind which is not untypical of the conditions in Amazonia (Bastable *et al.*, 1993).

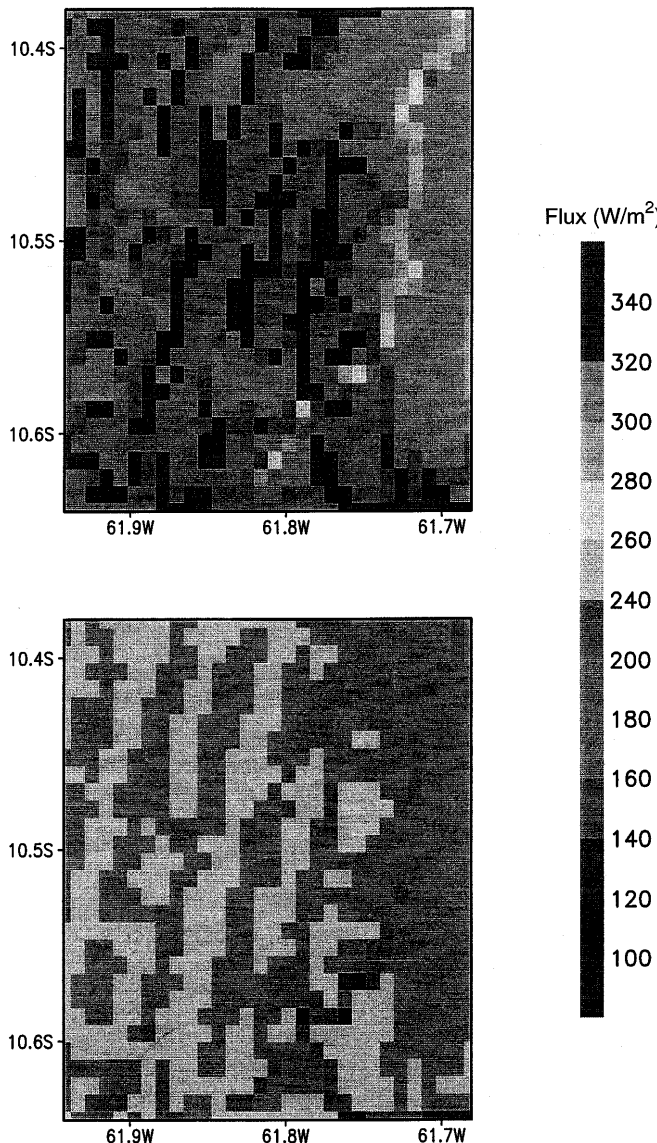


Fig. 11A, B. Diagrams of **A** latent and **B** sensible heat for the smallest domain of RAMS (Fig. 6)

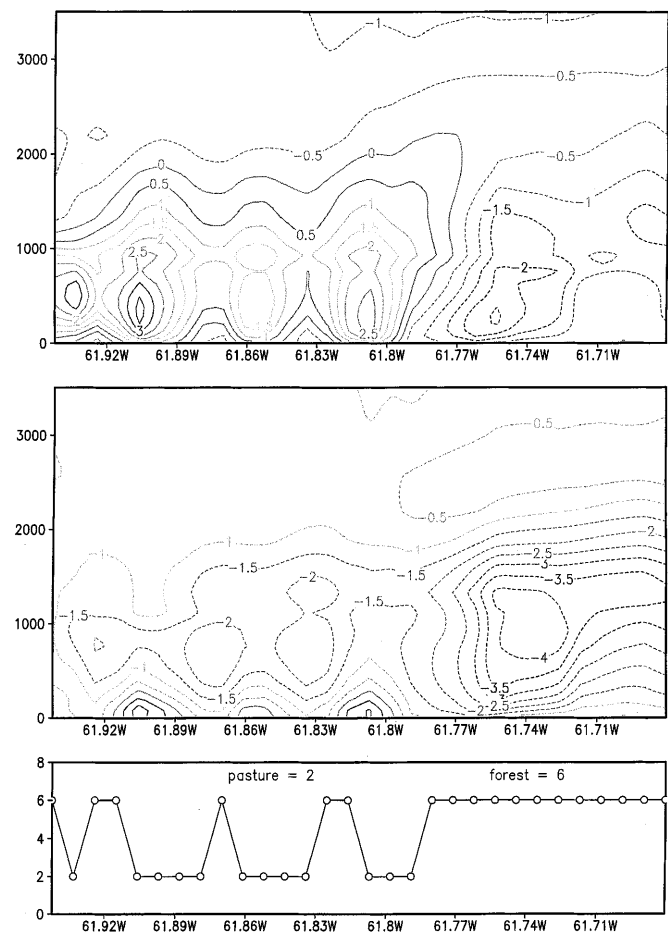


Fig. 12A–C. Cross section at 10° 6' S of vertical velocity (cm/s) at 20 August using RAMS at **A** 13.00 local and **B** 17.00 local time. **C** shows the land surface cover

sing that the level of the background wind will to a large extent determine the fate of the circulations. The current simulations are made with a background wind which is not untypical of the conditions in Amazonia (Bastable *et al.*, 1993).

Meso- β scale modelling

The RAMS model is also run with two grids centred at 15°S and 63°W, in central Rondonia with the first grid having a grid length of 60 km and the second of 20 km. The first grid covers the Amazon Basin plus the Andes Mountains the second covers only the Rondonian state. Simulations have been executed for 15–20 August, 1994, in the dry season using the NCEP analysis as initial condition and as boundary conditions updated every 12 h, with nudging at the 5 most exterior gridpoints and with time scales similar to those used in the meso γ runs. Vertical resolution starts at 300 m close to the surface and gradually decreases to 1000 m and remains fixed at this value up to model top at almost 20 km above sea level, using a total of 25 vertical levels. The land surface in this case is covered by evergreen forest only.

From the simulations performed, two examples will be used here to indicate the possible impact of the Andes Mountains in the atmosphere over Rondonia in the dry season. Note that even if the convection parametrisation was turned on, no modelled convection is triggered over Rondonia, in accordance with the satellite images of the period which showed total absence of cloudiness over the region. Only a few spots of cloudiness are observed, in the model simulations and in the satellite images, in the northern part of the Amazon Basin.

Simulations of the circulation in a zonal cross section, in grid 1, for August 17, 1994, at 1800 UTC are shown in Figure 13a (u component) and b (vertical component). Local time is 14.00. The outline of the Andes may be seen in these figures, while the centre of the domain is at 15°S and 63°W.

The figure shows that the circulation due to the Andes is quite strong, and generates vertical velocities of the order of almost $30 \text{ cm} \cdot \text{s}^{-1}$ close to the eastern slopes. The return circulation reaches a few hundreds of kilometres to the east of the eastern mountain top in

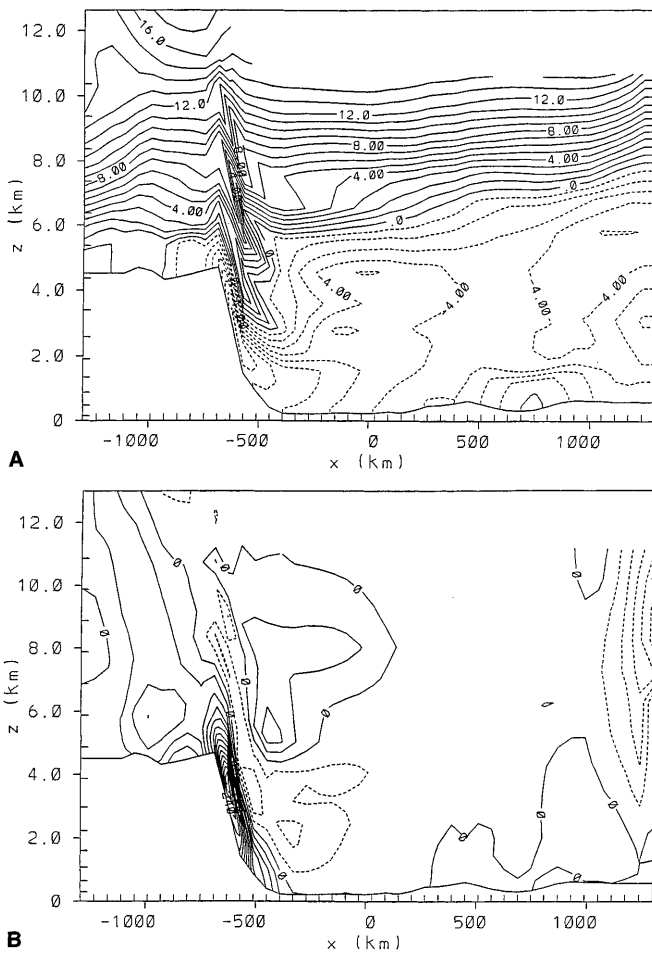


Fig. 13. **A** Zonal component and **B** vertical component of the wind field in a vertical cross section, for August 17, 1994, 1800 UTC. Cross section taken at 30 km north of the centre of the domain. Topography outline at the bottom. Dashed lines indicate negative values. Iso lines at every $1 \text{ m} \cdot \text{s}^{-1}$. Simulation started on August 15, 1994, 12 UTC

Fig. 13a, and the induced subsidence even further east. The region over central Rondonia experiences vertical velocities of $5 \text{ cm} \cdot \text{s}^{-1}$ at about 1500 m above sea level. This Andes induced subsidence (roughly 50 hPa/day) is important in suppressing the growth of the mixed layer over Rondonia and in maintaining the inversion strength in conjunction with the large-scale subsidence associated with the subtropical high pressure area.

The Andes also generates mountain waves in the current simulations. Figure 14a, b shows the simulations for August 19, at 1800 UTC and 600 UTC, for grid 2 with the 20 km grid length. While the afternoon simulation shows widespread subsidence over Rondonia in the lower and middle levels, the night time situation shows a pattern of gravity waves with a vertical wavelength of about 6 km. The horizontal wavelength is of the order of 250 km. Theoretically these can be classified as inertia-gravity waves with almost horizontal propagation. The implications of the existence of these waves for the vertical transport of atmospheric constituents is not certain. Maximum vertical speeds are of the

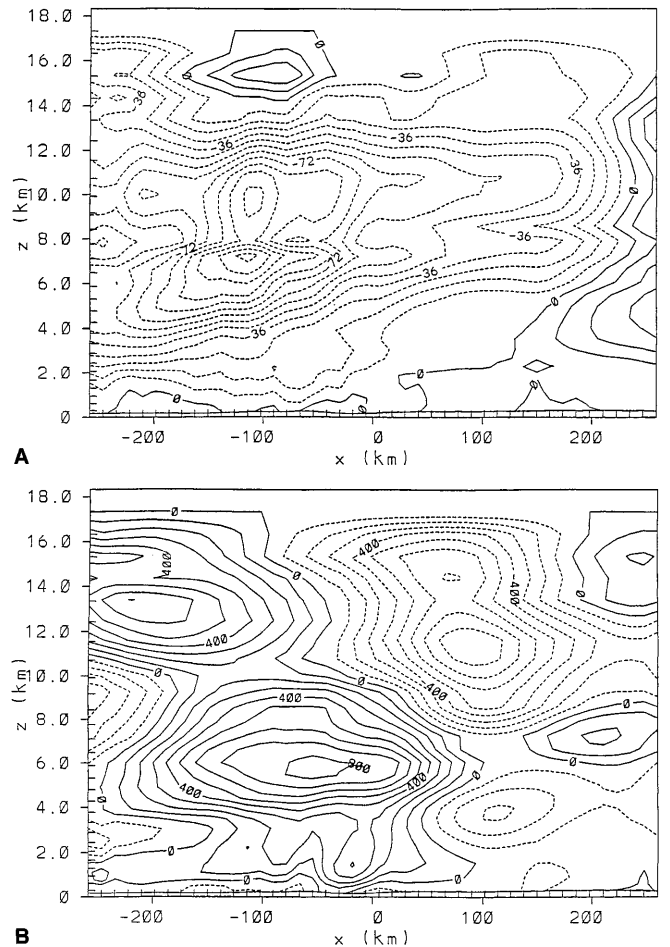


Fig. 14A, B. Vertical velocity in a vertical cross section, for August 19, 1994, at **A** 1800 UTC and **B** 600 UTC. Cross section taken at 6 km east of the centre of the domain. Topography outline at the bottom. Dashed lines indicate negative values. Iso lines at every $1 \text{ cm} \cdot \text{s}^{-1}$. Maximum value $8 \text{ cm} \cdot \text{s}^{-1}$, minimum value $-8 \text{ cm} \cdot \text{s}^{-1}$. Simulation started on August 17, 1994, 12 UTC

order of $8 \text{ cm} \cdot \text{s}^{-1}$. Acting over 4 h, these could imply a vertical displacement of air parcels of about 1000 m, upward or downward.

Other effects are also important and have been reported elsewhere. Figueroa *et al.* (1995) and Gandu and Geisler (1992) have shown that during the wet season the effect of the Andes is to channel the low level flow. This produces a southward current at low levels transporting moisture from the Amazon Basin towards mid-latitude South America. In the dry season, the climatological flow in Rondonia has a stronger eastern component, and meridional transport is not well defined.

Discussion and conclusions

The land surface models ISBA and RAMS are capable of adequately describing the partitioning of surface fluxes for the periods over which they were calibrated. This is slightly better for forest than for pasture, where soil moisture stress needs to be calibrated. The modelling of the development of the boundary layer is good-to-reasonable for forest areas. For pasture areas, where the ABL is observed to be up to 800 m deeper than over the forest, the model boundary layers are too cold and the final depths too low. The models are not able to reproduce the observed differences in temperature and depth of the ABL between forest and pasture. Adequate modelling of the fluxes from the land surface is required to provide the correct diurnal boundary layer forcing and thus considerable attention has to be paid to improve the current land surface schemes of meso-scale models (e.g. Ashby, 1999). A data collection program would also need to establish good measurements of surface temperature, soil hydraulic properties and particularly rooting depth (e.g. Delire *et al.*, 1998).

Given the importance of the boundary layer in transferring energy away from the surface into regions where it can be used to sustain convection, the disability of the models to predict the correct boundary layer growth and structure over pasture is particularly worrisome. This failure of the models inhibits realistic simulations of the effect of regional deforestation on the precipitation, both in the dry and the wet season. Furthermore, it is noteworthy that both the simple slab models (Nobre *et al.*, 1996b) as well as the more developed meso-scale models do not perform well over pasture.

Three possible reasons may explain this missing heat source. The models currently do not prescribe boundary layer heating through enhanced radiation absorption by aerosols, and also do not have sufficient extinction of shortwave radiation to predict the correct surface radiation budget. At present the effect of aerosols is taken into account by empirically adjusting the solar constant for RAMS by 15%, or in MESO-NH by assuming a boundary layer aerosol profile similar to that of humidity. The results from recent experiments suggest (Hobbs *et al.*, 1997) that the upward scattering albedo of smoke is of order 25%. This is of the same order of

magnitude as by which the solar input was reduced in the models. Simultaneous measurements of aerosol content and structure together with the boundary layer structure during the dry season campaign is the most important experimental requirement for LBA.

Secondly, the areas of pasture in the meso-scale model grids are in reality combinations of pasture and forest. This will increase the area grid box roughness length with respect to pure pasture, but may reduce the sensible heat input because of the lower surface resistance of the forest. It may well be that the lack of adequate mixing also hinders correct simulation of the boundary layer. An under prediction of the turbulence intensity for instance may, if it affects sub grid scale entrainment at the mixed layer top, also contribute to less heating. The precise mechanism of this is unclear but may be related to the contribution to the overall roughness of pasture areas by the remaining patches of forests and possible thermal circulations. This aspect needs to be further investigated by using a combination of boundary layer, tethered balloon, RASS and Sodar measurements at and around the forest/pasture interfaces. Low-flying flux aircraft will be needed to assess the lateral and vertical variation in momentum, and possibly sensible heat flux and other fluxes at the top of the boundary layer. To allow a correct determination of the different terms contributing to the heat budget of the boundary layer, accurate budget studies need to be executed consisting of several simultaneous radio-sonde releases over an area.

Thirdly, subsidence may contribute to boundary layer heating. However, subsiding air will also act to preserve the strength of the inversion and to suppress the growth of the boundary layer. The interplay between these two may result in warm but relatively shallow boundary layers. The simulations have relatively shallow boundary layers, but underestimate the total heat content and depth. Estimating the level of subsidence requires good large scale analyses, which ultimately depend on the quality and density of the radio sonde observation network over Amazonia. To be able to perform this analysis, considerable enhancement of this network is needed.

Topography also influences the flows. At the meso- β scale the influence of the Andes becomes important. Not only does large-scale subsidence in the dry season result from circulations induced by the Andes, the mountain range also generates gravity waves, which may have implications for transport of atmospheric constituents. The subsidence induced by the Andes circulations may also be important in suppressing boundary layer growth and convection in the dry season.

The ability of meso-scale models to simulate wet season conditions in the Rondonia area has not yet been adequately tested, largely due to the lack of observations of the wet season boundary layer. Initial model studies are required to investigate the effect of the surface on convection, in particular the effect of the effective aerodynamic roughness or enhanced turbulence of the surface coupled with the rapid recycling of intercepted water (Blyth *et al.*, 1993). Moreover, the parametrisa-

tions of entrainment, radiative absorption through aerosols need to be improved to realistically simulate dry season boundary layer development.

The model studies presented are attempts to show where our understanding of the interplay of local and continental scale mechanisms is not quite adequate. Above all, they show that the picture presented by GCM modelling studies needs to be balanced by an increased understanding of what happens at the meso- β and γ scales. LBA can provide this much needed understanding by addressing these questions with a number of coordinated field efforts, such as the wet season campaign planned for February–March 1999 in Rondonia.

Acknowledgements. The European contributions to this research were sponsored by the European Commission, Environment and Climate Programme, EV5V-CT94-0456 and the Ministry of Agriculture, Nature Management and Fisheries of the Netherlands. We would like to express our sincere thanks to the Institute of Hydrology for providing us with the very valuable and unique surface flux data set. The data were collected under the ABRACOS project and made available by the Institute of Hydrology (UK) and the Instituto Nacional de Pesquisas Espaciais (Brazil). ABRACOS is a collaboration between the Agencia Brasileira de Cooperacão and the UK Overseas Development Administration.

Topical Editor Y.-P. Duvel thanks J. Polcher and another referee for their help in evaluating this paper.

References

- Ashby, M.,** Modelling the water and energy balances of Amazonian rainforest and pasture using Anglo-Brazilian climate observation study data, *Agric. For. Meteorol.*, in press, 1990.
- Avissar, R., and Y. Liu,** Three-dimensional numerical study of shallow convective clouds and precipitation induced by land surface forcing, *J. Geophys. Res.*, **101** (D3), 7499–7518, 1996.
- Avissar, R., and R. A. Pielke,** A parametrisation of heterogeneous land surfaces for atmospheric numerical models and its impact on regional meteorology, *Mon. Weather Rev.*, **117**, 2113–2136, 1989.
- Bastable, H. G., W. J. Shuttleworth, R. L. G. Dallarosa, G. Fisch, and C. Nobre,** Observations of climate, albedo, and surface radiation over cleared and undisturbed Amazonian forest, *Int. J. Climatol.*, **13**, 783–196, 1993.
- Blyth, E. M., J. Noilhan, and A. J. Dolman,** The effects of forests on mesoscale rainfall: an example from HAPEX-Mobilhy, *J. Appl. Meteorol.*, **33**, 445–454, 1993.
- Bougeault, P., and P. Lacarrere,** Parametrisation of orography induced turbulence in a meso- β -scale model, *Mon. Weather Rev.*, **117**, 1872–1890, 1989.
- Bougeault, P., J. Noilhan, P. Lacarrere, and P. Mascart,** An experiment with an advanced land surface parametrisation in a mesobeta-scale model. Part I: implementation, *Mon. Weather Rev.*, **119**, 2358–2373, 1991.
- Calvet, J. -C., R. Santos-Alvalá, G. Jaubert, C. Delire, C. Nobre, I. Wright, and J. Noilhan,** Mapping surface parameters for meso-scale modelling in forested and deforested south-western Amazonia, *Bull. Am. Meteorol. Soc.*, **78**, 413–423, 1997.
- Cutrim, E., D. W. Martin, and R. Rabin,** Enhancement of cumulus clouds over deforested lands in Amazonia, *Bull. Am. Meteorol. Soc.*, **76**, 1801–1805, 1995.
- Delire, C., J. -C. Calvet, J. Noilhan, I. Wright, A. Manzi, and C. Nobre,** Physical properties of Amazonian soils – A modelling study using the ABRACOS data, *J. Geophys. Res.*, **102**, 30 119–30 133, 1998.
- Dolman, A. J., P. Kabat, J. H. C. Gash, J. Noilhan, A. M. Jochum, and C. A. Nobre,** A large-scale field experiment in the Amazon basin (LAMBADA/BATERISTA), in Ed. Troen, I., Climate change and impacts, European Commission, Brussels, pp., 789–796, 1993.
- Fisch, G.,** Camada limite Amazonica: aspectos observacionais e de modelagem, PhD Thesis, INPE/USP, Sao Jose dos Campos, Brazil, 1996.
- Fisch, G., C. A. Nobre, R. F. F. Lyra, A. D. Culf, E. J. P. Rocha, H. R. Rocha,** Observational aspects of atmospheric boundary layer developed over tropical forest and pasture in the Amazon region. To be submitted to *Bound. Lay. Meteorol.*, 1997.
- Figueiroa, N. F., P. Satyamurti, and P. L. Silva Dias,** Simulations of the summer circulation over the South American region with an eta co-ordinate model, *J. Atmos. Sci.*, **52**, 1573–1584, 1995.
- Gandú, A. W., and J. E. Geisler,** A primitive equation model study of the effect of topography on the summer circulation over tropical South America, *J. Atmos. Sci.*, **48**, 1822–1836, 1992.
- Gash, J. H. C., and C. A. Nobre,** Climatic effects of Amazonian deforestation: some results from ABRACOS, *Bull. Am. Meteorol. Soc.*, **78**, 823–830, 1997.
- Gash, J. H. C., C. A. Nobre, J. M. Roberts, and R. L. Victoria,** *Amazonian deforestation and climate*, Wiley, NY, 1996.
- Hobbs, P. V., J. S. Reid, R. A. Kotchenruter, R. J. Ferek, and R. Weiss,** Direct radiative forcing by smoke from biomass burning, *Science*, **275**, 1776–1778, 1997.
- Horel, J. D., A. N. Hahmann, and J. E. Geisler,** An investigation of the annual cycle of convective activity over the tropical Americas, *J. Clim.*, **2**, 1388–1403, 1989.
- Kirchhoff, V. W. J. H. (Ed.),** *SCAR-B Proceedings*, Transtec Editorial, San Jose dos Campos, Brazil, 1996.
- Klemp, J. B., and R. B. Wilhemson,** The simulation of three-dimensional convective storm dynamics, *J. Atmos. Sci.*, **35**, 1070–1096, 1978.
- Lafore, J. P., J. Stein, N. Asencio, P. Bougeault, V. Ducrocq, J. Duron, C. Fisher, P. Hereil, P. Mascart, J. P. Pinty, J. L. Rederlsperger, E. Richard, and J. Vila-Guerau de Arellano,** The MESO-NH atmospheric simulation system. Part 1A Diabatic formulation and control simulations. *Ann. Geophysicae*, **16**, 90–109, 1998.
- Lean, J., and P. Rowntree,** A GCM simulation of the impact of Amazonian deforestation on climate using an improved canopy representation, *Q. J. R. Meteorol. Soc.*, **119**, 509–530, 1993.
- Martin, C. L., D. Fitzjarrald, et al.,** Structure and growth of the mixing layer over Amazonian rain forest, *J. Geophys. Res.*, **93** D, 1361–1375, 1988.
- Mattos, L. F., C. P. Dereczynski, T. A. Tarasova, I. V. Trotsikov, and C. A. Nobre,** Brazilian contribution to SCAR-B project-meteorology, in *SCAR-B Proceedings*, Ed. Kirchhoff, V.W.J.H., Transtec Editorial, San Jose dos Campos, Brazil, pp. 145–148, 1996.
- Mohr, K. I., and E. J. Zipser,** Mesoscale convective systems defined by their 85-GHz ice scattering signature: size and intensity comparison over tropical oceans and continents, *Mon. Weather Rev.*, **124**, 2417–2437, 1996.
- Morcrette, J. J.,** Description of the radiation scheme in the ECMWF Model, *ECMWF Technical Memorandum 165*, Reading, 1989.
- Nobre, C. A., et al.,** *The large-scale biosphere atmosphere experiment in Amazonia (LBA), concise experimental plan*, CPTEC, Cachoeira Paulista, SC-DLO, Wageningen, 1996a.
- Nobre, C. A., G. Fisch, H. R. Rocha, R. F. Lyra, E. P. Rocha, A. C. L. Costa, and V. N. Ubarana,** Observations of the atmospheric boundary layer in Rondonia, in, *Amazonian Deforestation and Climate*, Eds. Gash J.H.C., Nobre, C.A., Roberts J.M. and Victoria R.L., J. Wiley & Sons, pp., 413–424, 1996b.
- Noilhan, J., and S. Planton,** A simple parametrisation of land surface processes for meteorological models, *Mon. Weather Rev.*, **117**, 536–549, 1989.

- Noilhan, J., P. Lacarre, A. J. Dolman, and E. M. Blyth,** Defining area average parameters in meteorological models for land surfaces with meso scale heterogeneity, *J. Hydrol.*, 302–316, 1997.
- Orlanski, I.,** A rational subdivision of scale for atmospheric processes, *Bull. Am. Meteorol. Soc.*, **56**, 527–530, 1975.
- Pielke, R. A., W. R. Cotton, R. L. Walko, C. J. Tremback, M. E. Nicholls, M. D. Moran, D. A. Wesley, T. J. Lee, and J. H. Copeland,** A comprehensive meteorological modelling system-RAMS, *Meteorol. Atmos. Phys.*, **49**, 69–91, 1992.
- Polcher, J.,** Sensitivity of tropical convection to land surface processes, *J. Atmos. Sci.*, **52**, 3143–3161, 1995.
- Silva Dias, M. A. F., and P. Regnier,** Simulation of mesoscale circulations in a deforested area of Rondonia in the dry season, in, *Amazonian Deforestation and Climate*, Eds. Gash J.H.C. , Nobre C.A., Roberts J.M. and Victoria R.L., J. Wiley & Sons, pp., 531–548, 1996.
- Skole, D., and C. Tucker,** Tropical deforestation and habitat fragmentation in the Amazon: satellite data from 1978–1988, *Science*, **260**, 1905–191, 1993.
- Sommeria, G., and W. Deardorff,** Subgrid-scale condensation in models of non-precipitating clouds, *J. Atmos. Sci.*, **34**, 344–355, 1977.
- Sud, Y. C., G. K. Walker, J. H. Kim, G. E. Liston, P. J. Sellers, and W. Lau, K-M.,** Biogeophysical consequences of a tropical deforestation scenario: a GCM simulation study, *J. Clim.*, **9**, 3225–3247, 1996.
- Wright, I. R., J. H. C. Gash, H. R. da Rocha, W. J. Shuttleworth, C. A. Nobre, G. T. Maitelli, C. A. G. P. Zamparoni, and P. R. A. Carvalho,** Dry season micrometeorology of central Amazonian ranch land, *Q. J. R. Meteorol. Soc.*, **118**, 1083–1099, 1992.